Quarterly Report for July - September, 1994
Kendall L. Carder, University of South Florida
NASS-31716

a) **Abstract**:

The algorithm-development activities at USF continue. We continue to refine our version 1 ATBDs(Algorithm Theoretical Basis Document) and a β version of pigment algorithm for use with MODIS data has been submitted to the Ocean Science team. We also finished a bio-optics cruise of the Florida Keys SE shelf.

b) **Task Accomplished**:

1. An R/V SUNCOASTER cruise was made from Tampa Bay to the Florida Keys Southeastern shelf area along the Florida west coast between July 26 and 29, 1994. Tasks included partitioning of the absorption coefficients of water samples, taking CDT and chlorophyll fluorescence profiles, and collecting remote sensing reflectance data and samples of bottom sediment. In-water optical measurements were made using SUDS (Spectral upwelling and downwelling spectrometer) by the 7 cruise participants.

2. Three β version of MODIS products were submitted to the EOS MODIS Project Ocean Science team:

2-1. Determining chlorophyll *a* concentration and gelbstoff of absorption coefficient for radiance data.

2-2. Calculating surface PAR(photosynthetically available radiation and IPAR(instantaneous PAR).

2-3. Calculating clear-water epsilons.

This new algorithm of 2-1 is an extension of the irradiance reflectance algorithm for [chl *a*] discussed in Carder et al. (1991). The major differences between the earlier algorithm and the present one occur in the particle backscattering and phytoplankton absorption terms. Given input $R_{rs}(\lambda)$ values, the algorithm first calculates the absorption coefficient due to phytoplankton at 675 nm, $a_\phi(675)$, and $a_g(400)$, and then [chl *a*] is calculated from the $a_\phi(675)$ value. $a_\phi(\lambda_i)$ for all MODIS wavebands centered at λ_i can then also be calculated from $a_\phi(675)$.

In principle, two spectral ratio equations can be used to solve for the two remaining unknowns, $a_\phi(675)$ and $a_g(400)$. Based on the shape of the absorption curve for phytoplankton versus those for CDOM and detritus, equations using spectral ratios of 412:443 and 443:555 for $R_{rs}(\lambda)$ should provide a good separation of the two absorption contributions. Signal-to-noise considerations may make it necessary to switch to other bands, but the philosophy behind the algorithm will remain the same. Once $a_\phi(675)$ is determined, $a_\phi(\lambda)$ for λ = 412, 443, 490, 510, and 555 nm can be estimated. The equations are solved using lookup tables (LUTs) (see Figures 1, 2).

The conversion of $a_\phi(675)$ to [chl *a*] requires a precise knowledge of the chlorophyll-specific absorption coefficient at 675 nm, $a^*_\phi(675)$. To avoid incomplete extraction problems, an expression for [chl *a*] as a function of $a_\phi(675)$ was developed using [chl *a*] values determined from the pigments extracted from the filter pad on which $a_\phi(\lambda)$ was measured and [chl *a*] was calculated from the *in vitro* samples using the methanol specific absorption coefficient of 0.0181 m^2/mg, which is a value determined in our lab on pure chlorophyll *a* from Sigma Chemicals. Substituting 0.0181[chl *a*] for $a_{\phi,MeOH}(666)$ in the regression equation

results in the following general equation for [chl *a*] as a function of $a_\phi(675)$

$$[chl\ a] = p_0 [a_\phi(675)]^{p_1} \quad (1)$$

where [chl *a*] is in mg/m^3 with the coefficients p_0 and p_1 equal to 61.9 and 1.012 for this version of algorithm.

Two sets of measured $R_{rs}(\lambda)$, [chl *a*], $a_\phi(675)$, and $a_g(400)$:

1.) from the subtropical data set;

2.) A low-light, high-nutrient data set was constructed consisting of stations from the MLML 1 and Tambax 2 cruises and of stations above 45° N from the TT010 cruise, were used to test the algorithm. Input $R_{rs}(\lambda)$ at the required MODIS wavebands were derived from hyperspectral $R_{rs}(\lambda)$ measurements and were weighted to simulate a 10 nm FWHM bandwidth. Measured [chl *a*], $a_\phi(675)$, and $a_g(400)$ were compared to modeled values, resulting in average fractional errors of 0.48, 0.38, and 1.03, respectively. The fractional error is calculated by

$$error = \exp\left[\frac{\sum_n |\ln(mod/mea)|}{n}\right] - 1 \quad (2)$$

where *mod* and *mea* are any of the modeled and measured quantities, respectively, and *n* is the number of data points.

It is encouraging that the [chl *a*] and $a_\phi(675)$ fractional errors are less than 0.5 for subtropical Pacific and Atlantic and high-latitude August data. Also encouraging is the fact that the optical portion of the algorithm performed equally well for the low-light, high-

nutrient data. Only one model parameter, p_0, which is related to $a_\phi^*(675)$, needed adjustment to make the [chl *a*] estimates for the low-light, high-nutrient data as good as those for the subtropical data. Nutrient-rich, light-limited cells are typically large and pigment-rich, resulting in lower chlorophyll-specific absorption coefficients. These stations were considered to be low-light because of a cloudy light-history prior to measurements. The algorithm was tested on this data set and the fractional errors for modeled vs. measured [chl *a*], $a_\phi(675)$, and $a_g(400)$ were 0.87, 0.42, and 0.57, respectively. The parameter p_0 was doubled to reflect the increased pigment packaging expected for low-light-adapted cells and the [chl *a*] error was reduced to 0.35. Output values of $a_\phi(675)$ and $a_g(400)$ are not affected by this change.

c) **Tasks Anticipated**:

Much more field data need to be acquired to better validate the algorithm parameters for varying regions and seasons. In order to derive [chl *a*], it is vital to predict how $a_\phi^*(\lambda)$ will vary. Thus, we must study the effect on $a_\phi^*(\lambda)$ of 1) light history, which may be related to season, latitude, and recent cloud-cover, and of 2) nutrient history, which is influenced by upwelling, river plumes, and offshore/onshore proximity. We have done extensive field work in the Gulf of Mexico and have developed a general scheme to describe the seasonal variations there: spring bloom, where $a_\phi^*(\lambda)$ is low and detritus is low; summer, where $a_\phi^*(\lambda)$ is high and detritus is increasing; and fall, where $a_\phi^*(\lambda)$ is high and detritus is high. This description should be applicable to other subtropical regions. We have cruises to the Arabian Sea planned for the summer and fall seasons, which will provide data sets for a coastal upwelling/high light regime to complement our continuing work in the Gulf of Mexico.

Future versions of the algorithm will include several flags to indicate exceptions such as

low $L_w(412)$ and possibly low $L_w(443)$ (i.e., a low signal-to-noise flag), high detritus and/or suspended sediments (possibly indicated by high $L_w(555)$), bottom reflectance, or cocolithophore blooms. For each flag, provisions can be made for switching to a flag-specific LUT.

d) **References cited**:

Carder, K. L., S. K. Hawes, K. A. Baker, R. C. Smith, R. G. Steward, and B. G. Mitchell, Reflectance Model for Quantifying Chlorophyll *a* in the Presence of Productivity Degradation Products, *J. Geophys. Res.*, 96(C11), 20,599-20,611, 1991.

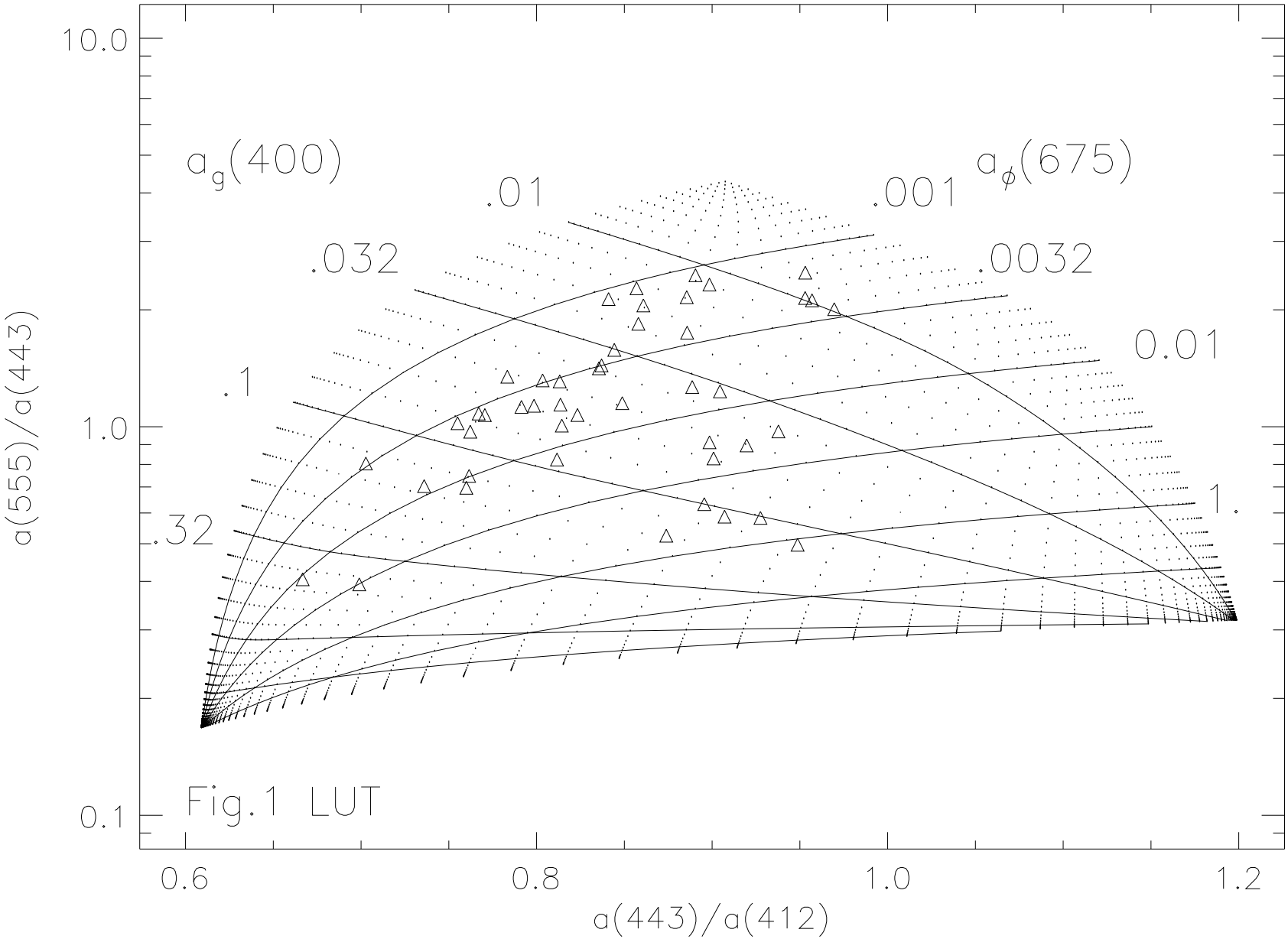
10.0
1.0
0.1
a(555)/a(443)
0.6
0.8
1.0
1.2
a(443)/a(412)
$a_g(400)$
$a_\phi(675)$
.01
.001
.032
.0032
.1
0.01
.32
1.
Fig.1 LUT

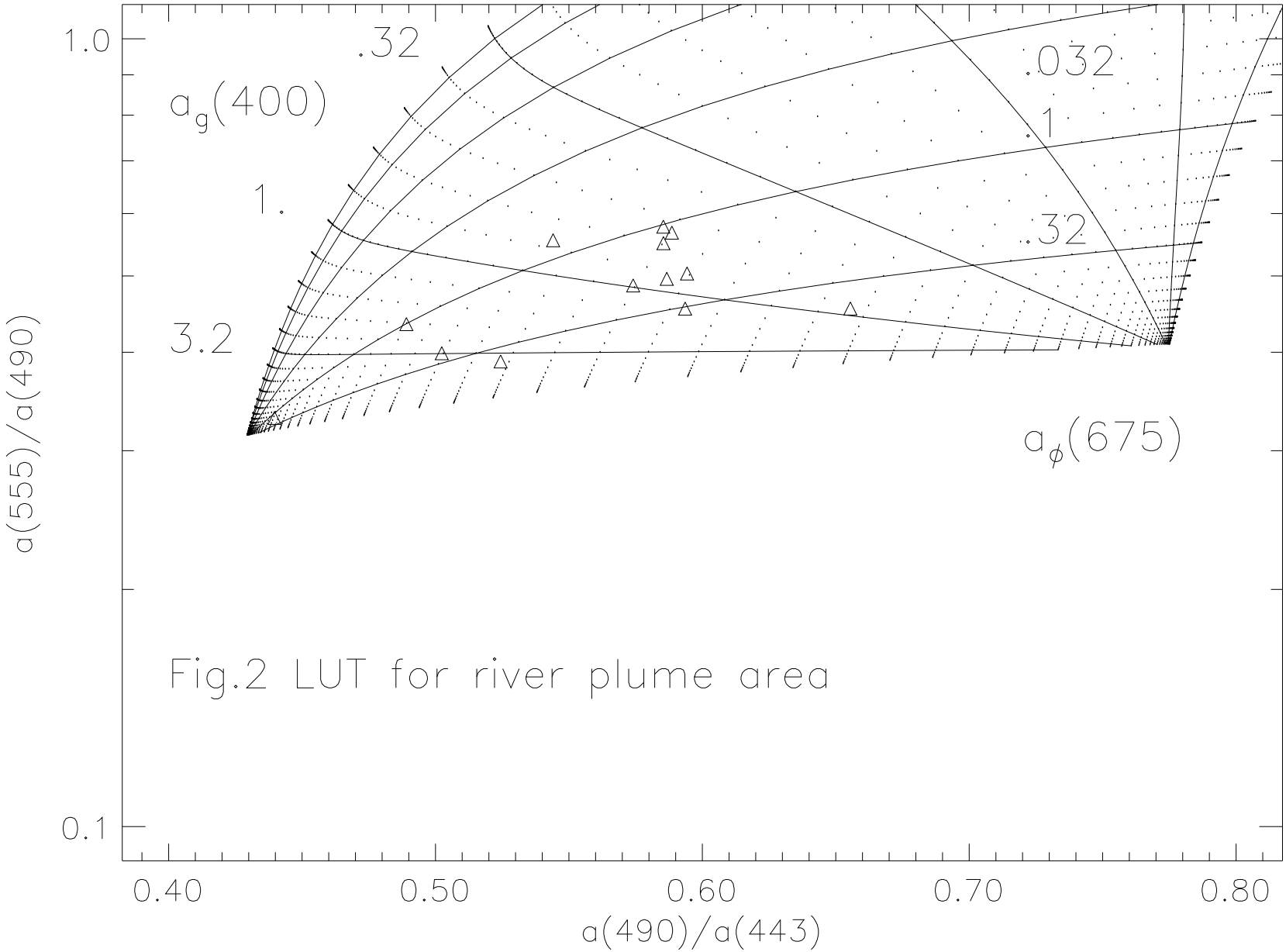

Fig.2 LUT for river plume area